The *Leptomonas collosoma* Spliced Leader RNA Can Switch between Two Alternate Structural Forms†

Karen A. LeCuyer and Donald M. Crothers*

Department of Chemistry, Yale University, New Haven, Connecticut 06511

Received November 12, 1992; Revised Manuscript Received February 10, 1993

ABSTRACT: We have used a combination of physical and molecular biological techniques to examine the structure of *Leptomonas collosoma* spliced leader RNA. We confirm the general features of the previously proposed structure for the 3′ half of the RNA, in which a single-stranded region is flanked by two stem loops. However, we find that the 5′ half of the RNA, which contains the splice site, has two competing secondary structures which differ only slightly in stability and which can interconvert on a fast (<1 s) time scale. In the favored conformation, a stable hairpin helix is augmented by conserved complementarity between the splice site and the 5′ end of the SL RNA. This putative helix has anomalous nuclease sensitivity and thermal stability features, suggesting that it is probably coupled by unknown tertiary interactions to other nucleotides in the 5′ half-molecule. The structure offers intriguing parallels with RNA–RNA interactions in the mammalian splicing system.

Pre-mRNA splicing is a process by which an intron is excised and the exons are then ligated [reviews: Padgett et al. (1986); Maniatis and Reed (1987)]; intermediates in the cis splicing reaction have been well characterized. The trans splicing reaction of trypanosomes and nematodes is a variant which involves the transfer of a 5′ exon (22–41 nucleotides long) from a short (<200 nucleotide) spliced leader transcript onto a preexisting mRNA (Konarska et al., 1985; Murphy et al., 1986; Sutton & Boothroyd, 1986). In trypanosomes all of the mature mRNAs contain the spliced leader at their 5′ ends. A trans spliced leader is also found in a small percentage of nematode mRNAs (Kraus & Hirsh, 1987; Blumenthal & Thomas, 1988).

The proposed secondary structure for the kinetoplastid spliced leader (SL) RNAs (Bruzik et al., 1988) was based upon relative free energies predicted by the Fold program (Zuker, 1989) and upon conservation of the folding pattern for several SL RNAs. This structural conservation among the trypanosomatid SL RNAs is striking due to the lack of length and sequence homology outside of the spliced leader exon portion of the molecule. The proposed secondary structure contains three stem loops, the second and third of which flank a single-stranded region which has the sequence of a binding site for Sm proteins (Mattaj, 1988). The latter are common splicing proteins that are immunoprecipitable by antibodies found in the serum of certain autoimmune patients (Lerner & Steitz, 1979). In vitro assembly of SL RNA snRNPs with HeLa cell Sm proteins, followed by immunoprecipitation with anti-Sm antibodies (Bruzik et al., 1988), shows that the putative Sm protein binding site of the SL RNAs is active in protein binding. U1 independence of splicing the trans spliced leader to an adenovirus exon in cis has also been demonstrated using U1-depleted HeLa cell extracts (Bruzik & Steitz, 1990). This result led to the proposal that the functional domain for 5′ splice site identification in trans splicing resides in the SL snRNP itself and not in a U1 RNA snRNP.

Our strategy for investigating the structure of the SL RNA begins with tests of the global features of the proposed model (Bruzik et al., 1988), primarily by determining the stability and binding kinetics of DNA oligonucleotides hybridized to the putatively single-stranded regions which are predicted by the model. This approach yielded the predicted results for the 3′ but not the 5′ half of the molecule. We also examined the thermal unfolding equilibria and kinetics for the molecule, using the temperature-jump (T-jump) technique, in which the sample is rapidly heated and the optical change is measured as a function of time. We found a low-temperature thermal transition which could not be accounted for by unfolding of helices in the model of Bruzik et al. (1988). Subsequent experiments localized this effect to the 5′ half of the molecule. We then employed mutagenesis and polyacrylamide gel electrophoresis methods such as ribonuclease mapping (Douthwaite & Garrett, 1981; Celander & Cech, 1990) and base modification/interference experiments (Peattie, 1979; Conway & Wickens, 1989; Weeks et al., 1990) to probe the structure of the 5′ half of *Leptomonas collosoma* SL RNA. We propose a new structure in which a stable hairpin helix is augumented by pairing of the 5′ end of the SL RNA with the splice site. The hairpin helix has a measured T_m about 6 °C higher than the analogous helix proposed by Bruzik et al. (1988). However, the putative splice site helix has unusual properties, including anomalously small thermal stability changes upon mutation, single-strand nuclease sensitivity at the splice site, and apparent tertiary interactions with additional nucleotides in the 5′ half of the SL RNA. We speculate that the internal splice site pairing may be analogous to pairing of the 5′ end of U1 with the 5′ splice site in mammalian pre-mRNA splicing (Zhuang & Weiner, 1986).

MATERIALS AND METHODS

DNA Oligonucleotides. All DNA oligonucleotides were synthesized on an Applied Biosystems 380B DNA synthesizer. Oligonucleotides <15 bases long were dialyzed into the buffer used for temperature-jump experiments. Oligonucleotides >15 bases long were purified on 10–15% denaturing polyacrylamide gels. Gel-purified DNAs were eluted in a Schleicher & Schuell elutrap device in 0.5× TBE buffer and

† Supported by Grants GM 21966 and AI 28778 from the National Institutes of Health and by the Yale MacArthur Center for Molecular Parasitology.

0006-2960/93/0432-5301$04.00/0

then ethanol precipitated and/or dialyzed before further experiments.

DNA Sequences. The DNA sequences used and their abbreviations are as follows: LCSM-8, 5′CCAAAATT3′; LCSM-10, 5′TCCAAAATTT3′; 3TLONG, 5′ATCCCCAAAGCCCGAAAGCTCGGTCCAAAA3′; 3TLONGB, 5′ATCCCCAAAGCCCGAAAGCTCGGTCCAAAATTTCAGAACTAGGTTCTG3′; 5TLONGB, 5′CTCTACATACCAATGAAGTACAGAAACTGTTCTTCAAAAATTGTTTTAGTT3′; FORM1SS, 5′GTCTCTACAT3′; 5TAILD, 5′GTTCTTCAAA3′.

RNAs. Full-length *L. collosoma* spliced leader RNA was made as a run-off transcript from a clone obtained from J. P. Bruzik and J. A. Steitz (Bruzik et al., 1988). RNAs were made using T7 RNA polymerase (a gift of either the P. B. Moore laboratory or R. Gregorian). For optical experiments 1–4-mL transcription reactions were used. Reaction conditions were as follows: 40 mM Tris, pH 8.1, 2 mM spermidine, 5 mM DTT, 40 mM $MgCl_2$, 4 mM each of rNTP, 0.1 mg/mL plasmid DNA linearized with Ba*m*HI and 0.1 mg/mL T7 RNA polymerase. Reactions were incubated at 37 °C for 4 h and then quenched with EDTA. Reactions were extracted once with an equal volume of 50/50 phenol/chloroform and twice with chloroform. The RNA was then ethanol precipitated, dissolved in a 50/50 mixture of water and formamide loading buffer, and purified on 10% denaturing polyacrylamide gels. Elution was performed in a Schleicher & Schuell elutrap device in 0.5× TBE for 3–4 h at 200 V. The RNA was removed from the elutrap and the optical density at 260 nm measured to calculate the concentration.

All other RNAs were made using oligonucleotide-directed transcription with T7 RNA polymerase (Milligan et al., 1987). The top strand contains −17 to +1 of the T7 promoter, while the bottom strand has the complementary bases to the top strand plus the remaining nucleotides of the RNA as a 5′ overhang. Reaction conditions are as follows: 40 mM Tris, pH 8.1, 1 mM spermidine, 0.01% (v/v) Triton X-100, 5 mM DTT, 80 mg/mL PEG, 4 mM each of rNTP, 30 mM $MgCl_2$, 300 nM annealed top and bottom strands, and 0.1 mg/mL T7 RNA polymerase. Reactions were incubated for 4–12 h at 37 °C depending on the stock of polymerase used. Reactions were then quenched, extracted, ethanol precipitated, run on 15% denaturing polyacrylamide gels, and eluted as above.

RNA Sequences. The sequence of the full-length SL RNA is as follows: 5′GGGAACUAAAACAAUUUUUGAAGAACAGUUUCUGUACUUCAUUGGUAUGUAGAGACUUCCAGAACCUAGUUUCUGAAAUUUUGGACCGAGCUUUCGGGCUUUGGGGAU3′.

The extra sequence added by the cloning procedure consists of a GGG at the 5′ end and a GGGGAU at the 3′ end. Because the RNAs are made by T7 RNA polymerase transcription, it was not possible to remove all of the extra G nucleotides from the 5′ end. We did, however, reduce the number of G's from 3 to 1 in one WT 5′ half-variant with no appreciable effect on its melting properties.

The WT RNA sequence is as follows: 5′GGGAACUAAAACAAUUUUUGAAGAACAGUUUCUGUACUUCAUUGGUAUGUAGAGACUUC3′.

The mutant RNAs are single or double base changes of the WT RNA and are designated as follows: M1, G to A at position 28; M2, G to A at position 20; C2, G to A at position 20 and C to U at position 40; M3, U to C at position 30; M4, C to G at position 6; M6, A to U at position 24; M7, U to C at position 7; M8, G to C at position 45; M9, G to C at position 44 and G to C at position 45; M10, G to C at position 44; /TA, 9 bases truncated from the 3′ end; TAM7, 9 bases truncated from the 3′ end and U to C at position 7.

Temperature-Jump Measurements. The T-jump apparatus is similar to that used earlier (Cole & Crothers, 1972), except that data are acquired using a LeCroy 6810 transient recorder and the LeCroy Catalyst software. Exponential curves are averaged and fit using the Asyst 3.0 software package. T-jump sizes ranged from 2–8 °C depending on the experiment. The amplitude of the relaxation is monitored at 266 nm and is plotted against the temperature corresponding to the midpoint of the temperature jump size. The total nucleic acid concentration ranged in absorbance from 0.5 to 2.

T-jump experiments were performed in TPSE7 buffer (10 mM Tris base, 50 mM monobasic sodium phosphate, 50 mM sodium sulfate, and 2 mM EDTA, pH adjusted to 7 with NaOH). RNA samples were ethanol precipitated and resuspended in TPSE7 buffer.

For the short DNA oligonucleotide probing experiments, the DNA was mixed with the RNA in a 2:1 ratio just prior to each experiment. For the long DNA oligonucleotide experiments, the DNA and RNA were mixed in a 1:1 ratio, heated to 70 °C, and slowly cooled to 4 °C. These RNA–DNA complexes were stable on native gels run at room temperature.

Native Polyacrylamide Gels. Native gels of RNAs were run in a Hoeffer constant temperature gel apparatus. The gels were 15%, 0.75 mm thick polyacrylamide gels run at 10 °C at 300 V until the bromophenol blue is at the bottom of the gel. The running buffer was 0.5× TBE, and the samples were renatured and preincubated at 10 °C in TPSE7 buffer. Gels were prerun for 1 h at 300 V and loaded while being run at 50 V.

5′ End Labeling of RNAs. RNAs were dephosphorylated with calf intestinal alkaline phosphatase (CIAP) (Boehringer Mannheim) and 5′ end labeled with T4 polynucleotide kinase (New England Biolabs) and [γ-^{32}P]ATP (NEN). After labeling, RNA was purified on 15% denaturing polyacrylamide gels and located by autoradiography. RNA was crushed and soaked in 0.5 M sodium acetate and 2 mM EDTA overnight at 4 °C. RNA was precipitated twice and resuspended in TPSE7 buffer.

Ribonuclease Mapping. Labeled RNAs were renatured in reaction buffer before incubation with the mapping enzymes. Ribonucleases T1 and P1 and cobra venom ribonuclease V1 (Pharmacia) were used at a variety of dilutions from 1/10 to 1/2000. Reactions were typically incubated at 4 °C for 2 min before being quenched with formamide loading buffer. The reaction buffer used is 5 mM Tris, pH 8.1, 60 mM NaCl, and 5 mM $MgCl_2$. Reactions were run on a 15% denaturing polyacrylamide gel, 40 cm long × 0.5 mm thick. Gels were run for approximately 2 h at 50–60 W. T1 sequencing reactions and hydroxide ladders were run as sequencing standards.

Modification/Interference. The base modification reactions were performed following standard protocols (Peattie, 1979; Conway & Wickens, 1989): reaction with hydrazine to give C>U and U modification and reaction with diethyl pyrocarbonate to give A+G modification. The modified RNA was run on a native gel as described above to separate form 1 from form 2 RNAs. After the RNA was crushed and soaked from the gel slices, it was precipitated and reacted with aniline to cleave at the modified bases. The reaction was extracted twice with butanol to remove the aniline. The RNA was washed with ethanol, dried, and resuspended in TPSE7 buffer. Formamide loading buffer was added, and the reactions were loaded on a sequencing gel as above. Unseparated modified RNA was both aniline cleaved and run on the sequencing gel

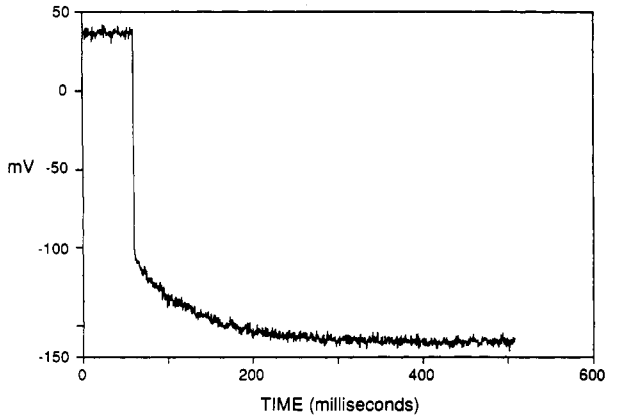

FIGURE 1: Typical T-jump trace for the SL RNA interacting with a short, complementary DNA oligonucleotide. This curve is the average of three traces taken at 12 °C for the LCSM-8 DNA oligonucleotide. The first 100 points represent the digitizer reading before it is triggered, the sharp drop reflects a rapid absorbance increase of the RNA which occurs upon rapid heating, and the exponential decay is the relaxation due to dissociation of the bound oligonucleotide. T-jump melting curves report the amplitude of the exponential decay observed on this time scale. Any RNA structural element whose melting relaxation time is as fast as or faster than the heating time, about 5 μs, will not contribute to these T-jump melting curves.

for comparison with the form 1 and form 2 RNAs.

Equilibrium Melting Curves. All equilibrium melting curves were taken automatically on a Varian Cary 1 spectrophotometer. Derivative melting curves were calculated and smoothed using the Asyst 3.0 software. All samples were heated to 70 °C for 3 min in the appropriate buffer and then slowly cooled to 5 °C before each melting experiment.

RESULTS

Probing the Full-Length SL RNA with DNA Oligonucleotides. This series of experiments involves the use of the temperature-jump (T-jump) technique to examine RNA structure [review: Turner (1986)]. This method has been used previously by our laboratory to study the secondary and tertiary structure of tRNA and bacteriophage R17 mRNA (Cole & Crothers, 1972; Gralla et al., 1974). In a T-jump experiment, an RNA sample at thermal melting equilibrium is displaced from that equilibrium by discharging a large capacitor across the T-jump cell. Absorption of the electrical energy causes an increase in sample temperature of a few degrees in a few microseconds. The data obtained are time-dependent decay curves of the RNA unfolding which are resolved into one or more exponential components. The amplitudes of the curves reflect the change in absorbance caused by the temperature-dependent unfolding, while the time evolution parameters reflect the intrinsic relaxation times (τ_i) for the melting process (Figure 1). The absorbance change is plotted for a series of temperatures to give a differential melting curve. Each maximum in the differential curve, at transition temperature T_m, reflects melting of one or more different elements of ordered nucleic acid structure. Bimolecular processes, such as hybridization of a DNA oligomer to an RNA, generally show relaxation times on the order of 100 ms near T_m, whereas unfolding of RNA secondary structural elements usually occurs in roughly 10–100 μs at T_m. Relaxation times for unfolding of tRNA tertiary structure have been observed in the 1–10-ms range (Cole & Crothers, 1972). Resolution of thermal melting curves on the time axis substantially increases their information content. The RNA variants examined were all T7 RNA polymerase transcripts with three guanosines added to their 5′ ends to increase

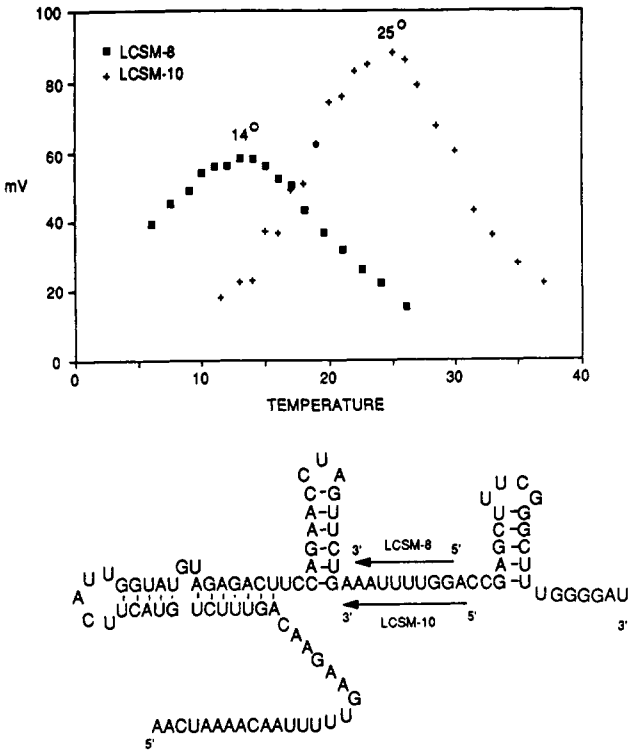

FIGURE 2: Interaction of the SL RNA with short DNA oligonucleotides LCSM-8 and LCSM-10, oligonucleotides complementary to the Sm binding site. The curves shown are the absorbance change due to the time-resolved part of the relaxation signal (Figure 1) (measured in mV), plotted against the midpoint of the T-jump size. The T_m of the complex is taken as the temperature of the maximum absorbance change. The SL RNA variants used contain an additional three G residues on the 5′ end to increase transcriptional efficiency. However, we found no systematic variation in transition properties when the number of G's was varied from 1 to 3. The full-length SL RNA transcript also has an additional GGGAU not present in the wild-type sequence at the 3′ end because of cloning restrictions.

transcriptional efficiency. (Equilibrium melting curve analysis demonstrates that RNAs with three 5′-guanosines have the same properties as those with just one 5′-guanosine that is essential for adequate transcriptional yields; data not shown.)

To examine SL RNA structure using the T-jump technique, 8–13 base long complementary DNA oligonucleotides were used as probes. SL RNA and a 2-fold excess of the DNA oligonucleotide were mixed in the T-jump cell, and the resulting melting profile was measured. If the DNA oligonucleotide binds to a region of the RNA which is accessible and thus single stranded, a melting profile with a large integrated absorbance change is observed. If, however, the DNA oligonucleotide is complementary to a region of the RNA which is bound in a preexisting RNA self-structure, the site will be inaccessible to oligonucleotide binding and a very small or no absorbance change will be seen. A series of short DNA oligonucleotides complementary to various regions of *L. collosoma* SL RNA were constructed.

The Sm binding site is a single-stranded region, as judged by secondary structure predictions and consensus with other Sm protein binding sites. Probing of the Sm protein binding site with the 8 base long LCSM-8 DNA oligonucleotide (Figure 2) gives a large amplitude T-jump signal with a T_m of 14 °C, suggesting that the Sm protein binding site is single stranded (Figure 2). The concentration dependence of the relaxation rate is also consistent with single-stranded character for the Sm binding site (data not shown). The LCSM-10 oligonucleotide, which should stack on the central helix of the proposed SL structure, gives an increase in T_m to 25 °C and a large absorbance change amplitude when compared to

LCSM-8. Thus, interaction of the SL RNA with oligonucleotides complementary to the putative Sm protein binding site confirms the single-stranded character of this region.

The Sm binding site and portions of the 3′ tail are the only sequences in the 3′ half of the molecule (defined as the Sm binding site plus the two helical stems which flank it) which give a signal consistent with a single-stranded region. Oligonucleotides complementary to helical stems 2 and 3 give no signal, a result consistent with the presence of these two helices (data not shown). Oligonucleotides complementary to the most 5′ single-stranded region give anomalous melting signals (see below), indicating that the structure in this region is more complicated than that in the Bruzik et al. (1988) model. In summary, probing the SL RNA with short DNA oligonucleotides confirms that the 3′ half of the RNA consists of two helical stems and two single-stranded regions, while the structure of the 5′ half of the SL RNA is not apparently consistent with the model.

Thermal Unfolding of the SL RNA. The T-jump differential melting curve for the full-length *L. collosoma* spliced leader RNA has two major amplitude maxima, one with a T_m of 35 °C ($\tau_m \sim 100$ μs) and one with a T_m of 62 °C ($\tau_m \sim 30$ μs), as indicated in Figure 3B. The low T_m of the first melting signal resembles observations for melting the tertiary structure of tRNA^{fMet} (Crothers et al., 1974), suggesting that tertiary structure should be included in the list of possible sources of the low-temperature transition in the SL RNA. The relaxation time of 100 μs is intermediate between the values that have been observed for melting of hairpin helices and tRNA tertiary structure. Upon closer examination, the higher T_m peak is asymmetric, suggesting that multiple melting processes may be occurring at high temperatures.

In order to identify the source of the signals in the melting curve of SL RNA, long complementary DNA oligonucleotides were synthesized and hybridized to regions of the RNA, thus eliminating the hybridized regions as sources of the melting signal measured for the hybrid (Figure 3A). (Stable hybridization was confirmed by electrophoresis of the hybrid; data not shown.) The 3TLONG oligonucleotide hybridizes to the most 3′ hairpin helix of the RNA and to the single-stranded regions on either side of it (Figure 3C). This alteration leaves the T-jump melting profile unaffected, leading to two conclusions: that the third helix is not responsible for the low-temperature transition and that we cannot directly measure a time-resolved melting signal for this helix. Because probing with small DNA oligonucleotides suggests the presence of this helix, we believe that either its T_m is too high or the melting kinetics are too fast to resolve with our instrument. Because equilibrium melting curves show no independent melting signal for this helix up to 95 °C, we favor the fast melting kinetics explanation.

The oligonucleotide 3TLONGB hybridizes to the most 3′ helix as does 3TLONG but is extended to include the central helix (Figure 3D). Hybridizing this oligonucleotide leaves the 33 °C signal intact, and even slightly stabilized, while removing the upper half of the 62 °C signal. Although the 33 °C signal is stabilized by ~4 °C, the unchanged relaxation time suggests that the structure is largely unperturbed. The increase in T_m may be due to additional stacking interactions introduced by the hybrid helix. Since the 3TLONGB complex lacks the upper half of the 62 °C signal, the melting of helix 2 is assigned to that region of the melting curve. When oligonucleotide 5TLONGB was hybridized to the RNA 5′ half nearly up to the start of helix 2 (Figure 3E), both the 33 °C signal and the low-temperature half of the 62 °C signal disappeared. The 5′ half of the SL RNA is thus the source

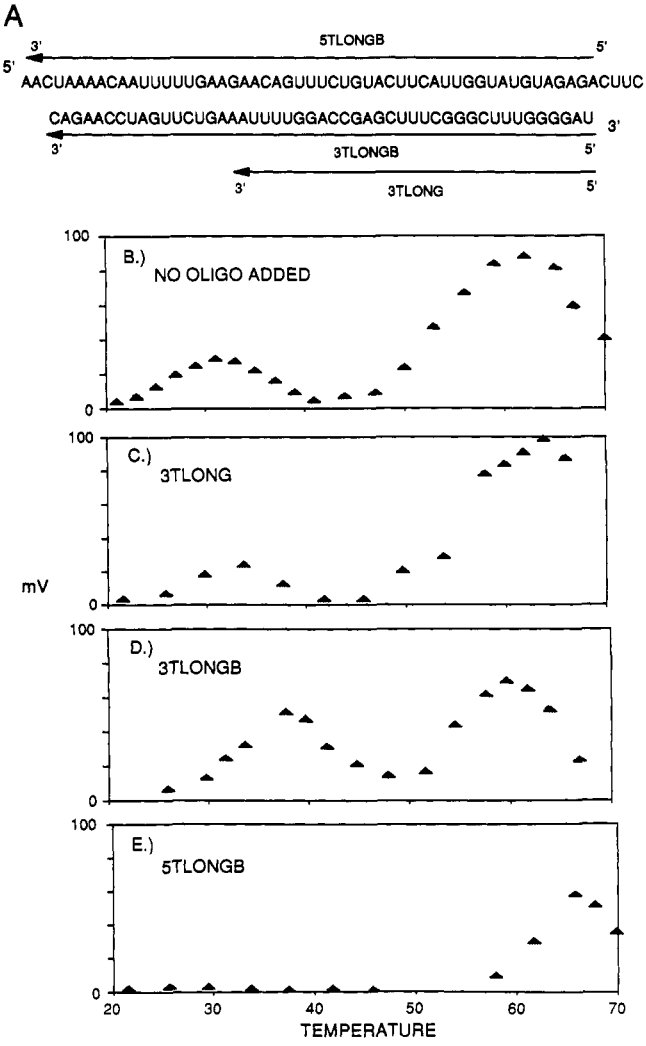

FIGURE 3: Suppression of melting signals by interaction of the SL RNA with long DNA oligonucleotides. (A) Arrows represent the oligonucleotides used in this experiment. The DNA sequences are complementary to the RNA sequences in the region covered by the arrows. (B) Differential melting curve of the intact SL RNA. Two melting signals are seen, one with a T_m of ~33 °C and one with a T_m of 58 °C. The relaxation times of the two signals at their T_m's are approximately 100 and 30 μs, respectively. (C–E) Differential melting curves for the SL RNA hybridized to oligonucleotides 3TLONG, 3TLONGB, and 5TLONGB. The curves represent the portion of the RNA which is not hybridized to the DNA oligonucleotide.

of the low-temperature melting signal, possibly arising from tertiary structure, as well as a signal corresponding to at least one hairpin helix.

The results obtained to this point showed little kinetic or equilibrium perturbation of the melting signals of the 5′ half-molecule by removal of all RNA structure from the 3′ half. These results led us to conclude that the 5′ and 3′ halves of the SL RNA are essentially structurally independent. Subsequent experiments were therefore done on a truncated RNA containing all of the 5′ sequence up to the beginning of helix 2, because this RNA contains the unknown putative tertiary structure as well as the crucial splice site for the trans splicing reaction. The melting profile of the SL 5′ half contains the expected melting signals of T_m ~35 and ~58 °C, as described below; equilibrium melting curves on 5′ half-molecules yielded a slightly higher T_m value for the 33–35 °C transition, by about 2 °C, than the T-jump curves taken on the whole molecule.

Mutagenesis of the L. collosoma SL RNA 5′ Half. Nondenaturing Gel Electrophoretic Mobility. Having lo-

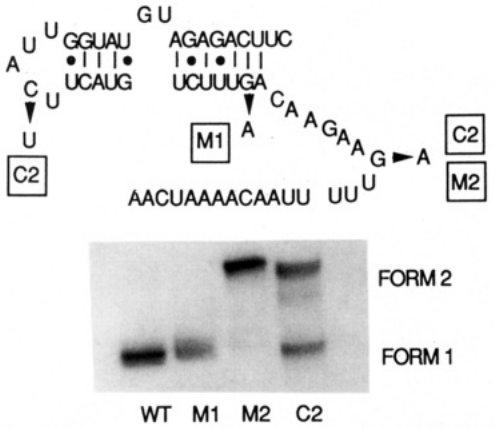

FIGURE 4: Point mutants made to examine the SL RNA 5′ half-structure and their native gel mobilities. Variant M2, which should have the same mobility as WT for the model shown, has a strikingly different gel mobility than WT RNA, while M1, which should have a destabilized structure, has an unaltered gel mobility. Compensating the mutation in M2 with the double mutation in C2, thus probing for a potential pseudoknot interaction, yields a nearly equal balance between the two different mobility species.

calized the 35 °C T-jump melting signal to the 5′ half of the SL RNA, we began to construct point mutants to further define the structure. The wild-type 5′ half-sequence is denoted as WT. Mutant M1 was designed to disrupt helix 1 in the Bruzik et al. (1988) structure. Mutant M2 was designed to probe a potential base-pairing (pseudoknot) interaction between the single-stranded region shown as M2 and the first three bases in the hairpin loop at C2 (Figure 4); this potential base pairing is conserved for all of the known trypanosomatid SL RNA sequences. When these RNAs are run on native polyacrylamide gels at low temperature, we observe that WT and M1 have the same electrophoretic mobility, while M2 moves much more slowly (Figure 4). This marked difference in electrophoretic mobility of WT and M2 led us to hypothesize that there are two forms of the SL RNA, the faster mobility structure which we call form 1 and an alternate structure favored in the M2 mutant, which we call form 2. Mutant C2, which contains a compensatory C to U change combined with the A to G change of M2, shows bands of both mobilities, suggesting that for C2 there is a balance between the two structures.

Modification/Interference. The difference in electrophoretic mobility of the two forms of the SL RNA was used in an application of the modification/interference technique of structure probing. Since single base changes affected the tendency of the RNA to fold into form 1 or form 2, single base modification might have a similar effect. In this experiment, labeled RNA was subjected to the A+G, C+U, and U chemical modification reactions (Peattie, 1979; Conway & Wickens, 1989). Modified RNA was run on a native gel, the bands corresponding to form 1 and form 2 were isolated, and the aniline reaction was used to cleave the RNA at the modified bases. RNAs of mobility corresponding to forms 1 and 2 were run separately on a sequencing gel and compared to RNA which was modified and cleaved but not separated into the two forms. Cleavages which are enhanced for either form 1 or form 2 when compared to the unseparated RNA are highlighted on the gel (Figure 5A). Bases which are enhanced in cleavage for form 2 are more important for form 1 structure than for form 2, and vice versa for base cleavages which are enhanced in form 1.

The results are summarized in the two secondary structure models for the 5′ half-molecule shown in Figure 5B. Enhanced cleavage seen in the form 1 and form 2 lanes generally

Table I: Comparison of the Potential Splice Site Helix Base-Pairing Interactions for Several Organisms

organism	splice site helix
	↓
L. collosoma,	UUGGU
C. fasciculata,	AAUCA
T. cruzi	A 5′
	↓
C. elegans	GAGGUA
	AUUUGG
	5′
	↓
S. mansoni	AUGGU
	UGCCA
	A 5′
	↓
E. gracilis	UUCGGUA
	GAGUCUU
	U 5′

corresponds to the proposed helical regions. The form 2 or mutant M2 structure is that found in the Bruzik et al. (1988) model. The wild-type structure (form 1) is a new model which contains an alternate hairpin helix, along with base pairing between an ACUAA sequence at the 5′ end and the UUGGU sequence at the splice site. These results indicate that the most stable structure for the wild-type 5′ half of the *L. collosoma* SL RNA is not that predicted by the Fold energy minimization program. The Fold program gives form 2 as the more stable structure by approximately 1 kcal/mol over form 1. Note that position C29, whose modification destabilizes form 2, is the end base pair in the GUUUC hairpin helix loop in form 1. Presumably its position next to a small loop makes its pairing less important for form 1 than it is for form 2, where it is internal to a helix. An analogous position dependence may account for the differential effect of modification of C34, which is more destabilizing for form 1 than for form 2.

Potential base pairing between the splice site and the 5′ end is conserved for all of the known trypanosomatid SL RNAs as well as those of the nematodes, trematodes, and *Euglena* (Takacs et al., 1988; Rajkovic et al., 1990; Tessier et al., 1991), if allowance is made for an A·G pair at the end of the helix in the case of *Caenorhabditis elegans* (Table I).

Evidence supporting the Bruzik et al. (1988) model for the SL RNA 5′ half includes conservation of the structure for all of the trypanosome SL sequences. However, all the SL RNAs can be folded into the newly proposed form 1 structure as well (Figure 6). The most variable portion of the sequence forms the multibase bulge near the 5′ end of the molecule, of sequence N-Pu-C-N_{3-6}. The conserved C in this loop is one of the nucleotides whose modification decreases the stability of form 1 relative to form 2 (Figure 5). We note in addition that *Crithidia fasciculata* SL RNA gives a T-jump melting profile and ribonuclease mapping pattern similar to that observed for *L. collosoma* SL RNA (data not shown), suggesting that the trypanosome SL RNAs in general may share the properties which we have characterized.

Ribonuclease Mapping. Nuclease mapping was performed using P1 and T1 nucleases as single-stranded probes and V1 nuclease as a double-stranded probe. Distinctive mapping patterns were observed for WT, a form 1 RNA, and M3, a form 2 variant (Figure 7A). For form 1 RNAs, V1 cutting is seen in the form 1 stem (bases 18, 19, and 36), in the putative splice site helix (bases 4 and 5), and in the A-U-rich bulge loop (bases 10 and 11) (Figure 7B). The cuts in the loop

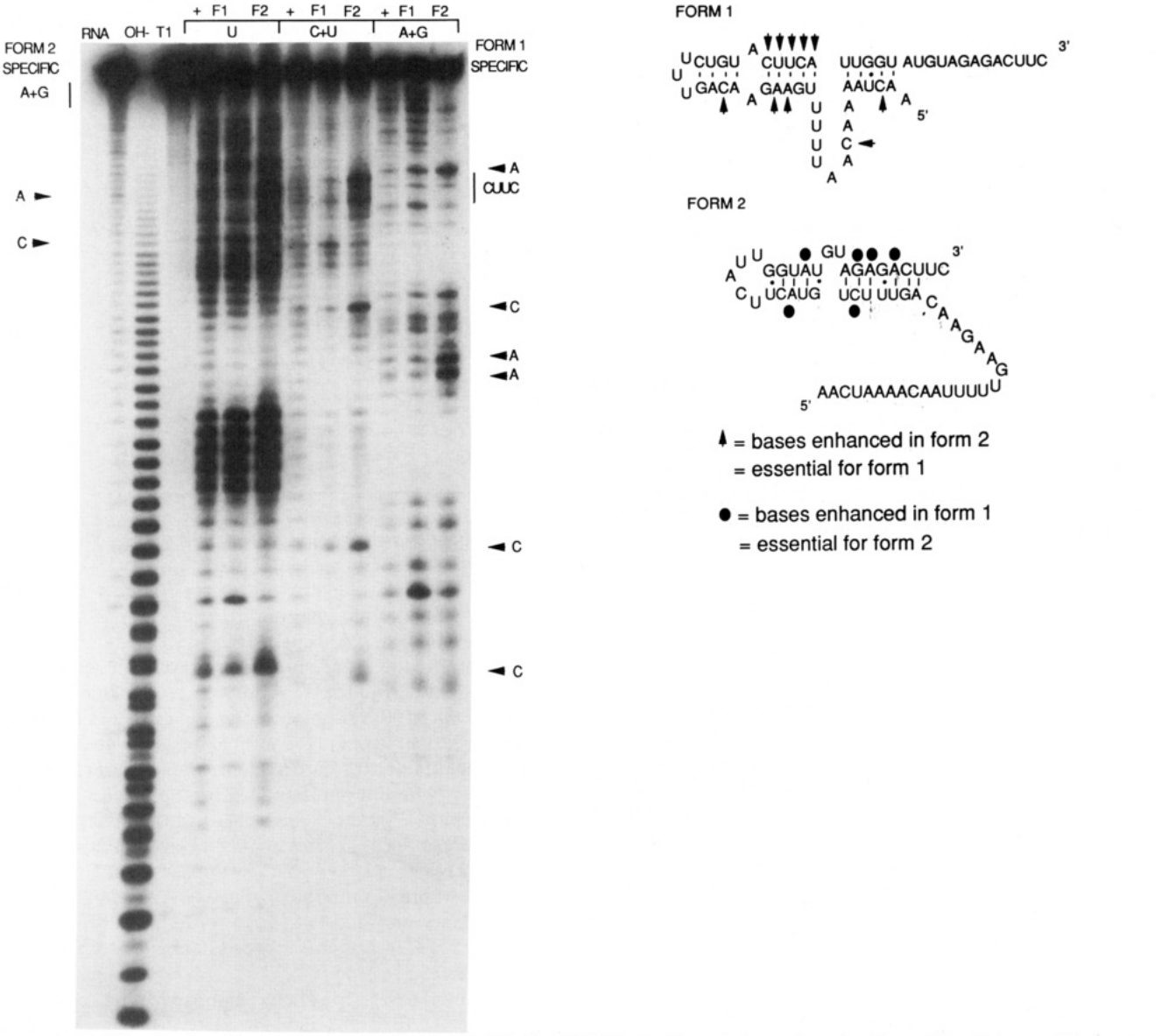

FIGURE 5: Modification interference results for the SL 5′ half. (A, left) Denaturing gel electrophoresis after aniline cleavage. Lanes are as marked: C+U, U, and A+G reactions were performed. An OH^- ladder and a T1 sequencing lane were used as markers. For each reaction, form 1 (F1), form 2 (F2), and unseparated (+) RNA lanes are shown. Cleavages strongly enhanced for either form 1 or form 2 when compared to the unseparated RNA are shown. (The cleavages highlighted are those which were strongly enhanced in repeated experiments.) The form 1 specific cleavages, noted on the right gel margin, occur at C3, C9, A18, A19, C23, CUUUC34–37, and A38, counting upward from the 5′ end (bottom) of the gel. The form 2 specific cleavages, indicated in the left gel margin, are observed at C29, A33, A44, G49, A50, and A52; the last four of these are marked A+G, reflecting the distinctly greater cutting in the A+G F1 lane than in the F2 lane in the top part of the gel. Note that the RNA chemical sequencing reactions do not yield clean 3′-terminal phosphate groups, in contrast to chemical sequencing of DNA, but produce instead terminal phosphodiesters which migrate anomalously slowly. Hence the hydroxide cleavage ladder is not a reliable marker for oligonucleotide fragment size. (B, right) The two forms of the SL RNA as indicated by the modification interference experiment, showing the cleavage sites indicated in (A). Regions of enhanced cleavage for the two forms are generally in the putative helical regions.

suggest that the bases it contains are either stacked or involved in an as yet unidentified structure. T1 and P1 nucleases cleave form 1 across the splice site and in the single-stranded region adjacent to the splice site at bases 41–43, 46, 49, and 50. This result suggests that the general structure of form 1 at the proposed splice site helix is not a stable canonical helix but that there may be some higher order structure which is somehow accessible to the single-strand-specific nucleases. Alternatively, the helix may be sufficiently unstable that its transient opening leads to cleavage. For form 2 RNAs, V1 cutting is observed in the helical stem region (bases 24–26, 30, and 50) as well as near the 5′ end (bases 4, 5, 10, and 11). The bases at the 5′ end may be stacked or interacting to form tertiary structure. T1 and P1 nucleases cleave form 2 primarily in single-stranded (bases 15, 16, 18, and 19), looped (bases 38 and 39), and bulged regions (base 46), with one unexplained cut in the helical stem (base 41). Thus the ribonuclease mapping data generally support the proposed secondary structures for the two forms, but there are indications for additional and modified structural elements.

Melting Curves for Mutants in the Core Helices. An equilibrium melting curve analysis was performed on several SL RNA 5′ half-variants with alterations in the stable core helices of forms 1 and 2 (Figure 8A). The data are displayed as the derivative of the absorbance versus temperature. The derivative melting curve for the WT 5′ half has melting signals at 35 and 58 °C. These signals were unaffected by reducing the number of extra G's at the 5′ end of the molecule to one. The 35 °C signal is differentially stabilized by the addition of Mg^{2+} when compared to the 58 °C signal: upon addition

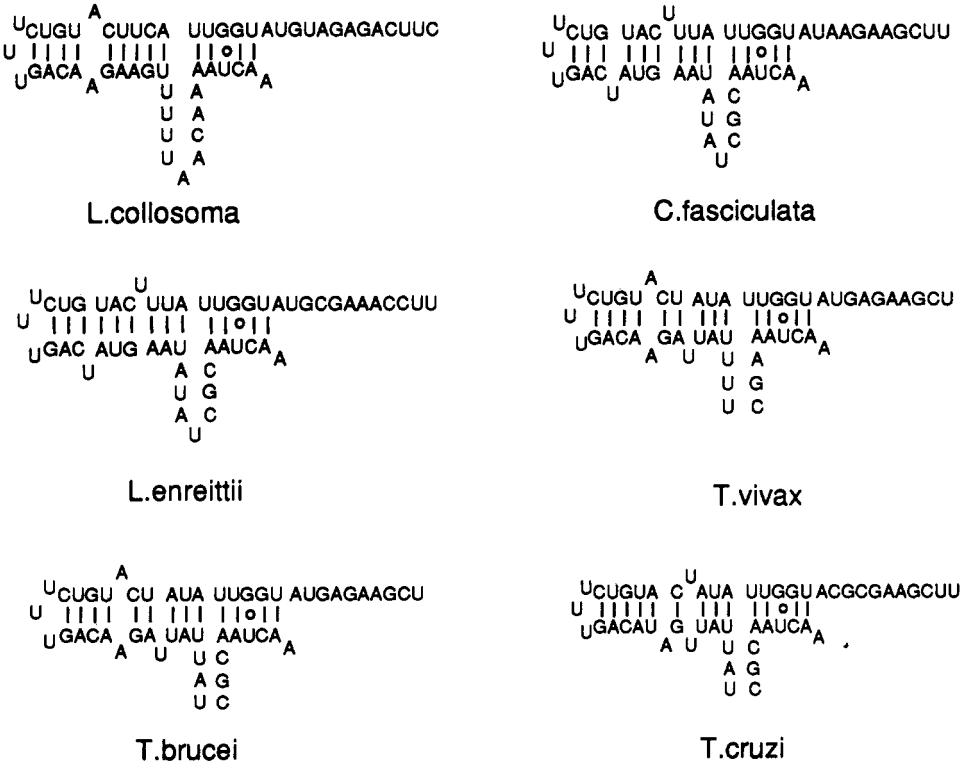

FIGURE 6: Form 1 secondary structure folding for the known trypanosomatid SL RNA sequences.

of 1 mM $MgCl_2$, the change in T_m for the low-temperature transition is 17 °C, while that for the high-temperature transition is 8 °C. This result supports the assignment of tertiary structural elements to the form 1 signal at 35 °C, whereas the 58 °C signal has the properties expected for melting of a helical region. The characteristic 35 °C transition is replaced by a smaller transition with a T_m of about 25 °C in form 2 mutants.

The effect of mutations on the temperature of the upper transition can be readily understood in terms of their expected effect on complementarity in the competing helices in forms 1 and 2. The derivative melting curve for M2, a mutant characterized as form 2 by its electrophoretic mobility and ribonuclease mapping pattern, has a single helix melting signal at 52 °C. Conversion of a G·C pair in WT to A·C in M2 destabilizes the form 1 secondary structure sufficiently to make form 2 more stable than form 1. This result establishes 52 °C as the melting temperature for the form 2 secondary structure. The ΔT_m of ≈6 °C compared to wild-type RNA gives a measure of the relative stabilities of the two competing secondary structures. The ΔH of the form 1 helical stem is estimated from the transition width to be 50 kcal/mol while that of the form 2 stem is 60 kcal/mol. The $\Delta\Delta G$ at the T_m between the two forms is approximately 1 kcal, and the equilibrium constant favoring form 1 is 5–6 near the T_m.

The double mutant C2, a derivative of M2, displays the characteristics of both of the RNA forms, as demonstrated by native gel analysis and by ribonuclease mapping. Mutant C2 can be regarded as a form 1 mutant which is destabilized by changing a G·C base pair to an A·U. The melting curve for C2 has a decreased amplitude for the tertiary structure melting and a decreased T_m for helix melting (55 °C). The mutant C2 is apparently in equilibrium between the two structural forms. The observed melting transition probably includes contributions from the characteristic melt (T_m = 52 °C) of the form 2 helix, leading to overlap of the signals for helix melting of the two forms. (The electrophoresis experiment shows, however, that the switch between the two forms is slow in gels at low temperature.)

Melting curves for several other core helix mutants have been analyzed (Figure 8A). Mutant M6 is a form 1 variant in which the A-A mismatch of the form 1 helical stem is repaired to an A·U base pair. The 35 °C signal is unaffected, showing that the "tertiary structure" signal is independent of the major melting signal for the helical stem, which is stabilized to 75 °C. This result confirms that the 35 °C signal is characteristic of RNAs which have the form 1 secondary structure. The observed stabilization of the M6 upper transition is consistent with its assignment to the helical region. Mutant M3 was characterized as form 2 by electrophoretic properties; its form 2 helix is stabilized by changing a G·U base pair to a G·C base pair, increasing T_m from 53 to 67 °C.

Mutations in the "Splice Site Helix". Mutant /TA RNA is a form 1 RNA which has nine bases truncated from its 3′ end (Figure 8B). The melting profile for this RNA has a small, broad low-temperature melting signal and a normal helix melting signal of T_m = 58 °C. This result suggests that the 3′ single-stranded region of form 1 RNA has a role in forming the tertiary structure. We believe that the small low-temperature signal for /TA may correspond to melting of the splice site helix alone. This tentative assignment is consistent with the properties of mutant M7, a form 1 RNA in which the G·U across the splice site has been changed to G·C, thus stabilizing the base pairing at the splice site. The low-temperature signal for this mutant is broadened, suggesting that it is composed of overlapping signals, one of which is stabilized and the other destabilized from the normal low-temperature melting behavior. When combined with the results for /TA, the M7 results suggest that the stabilization of the putative splice site helix has separated its melting from that of the destabilized tertiary structure.

This assignment was further tested by construction of a mutant designed to remove tertiary structure and stabilize the splice site helix. Mutant TAM7 is truncated as /TA with the G·U to G·C change incorporated at the splice site (data not shown). In this mutant the only low-temperature melting signal is seen as a shoulder on the 58 °C signal (data not

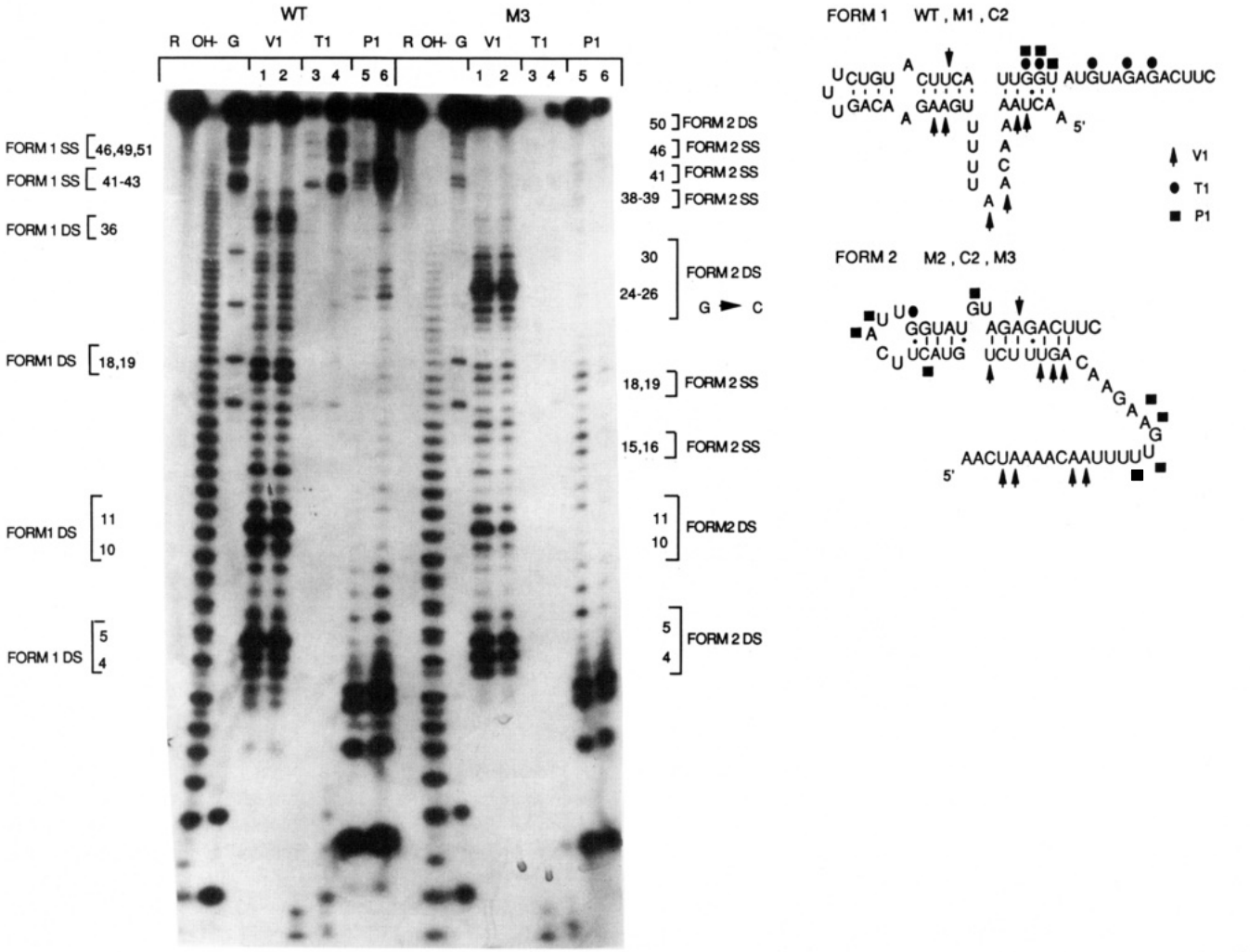

FIGURE 7: Ribonuclease mapping results for form 1 and form 2 RNAs. (A, left) Distinctive ribonuclease mapping patterns are seen for form 1 WT RNA (left panel) and the mutant form 2 M3 RNA (right panel) (G→C shows the site of mutation in M3). Labels are as follows: R = RNA, OH^- = hydroxide ladder, G = T1 sequencing lane, V1 = cobra venom ribonuclease, T1 = T1 ribonuclease, and P1 = P1 nuclease. Concentrations: 1 = 1 unit of V1 in 400 μL, 2 = 1 unit of V1 in 200 μL, 3 = 10 units of T1 in 5 μL, 4 = 10 units of T1 in 20 μL, 5 = 8 units of P1 in 500 μL, and 6 = 8 units of P1 in 1500 μL. Strong cleavages with V1, T1, and P1 nucleases are marked. FORM 1 DS are V1 nuclease cleavages enhanced for form 1, while FORM 1 SS are single-stranded T1 and P1 cleavages enhanced for form 1. FORM 2 DS and FORM 2 SS are the analogous cleavages for form 2. (B, right) The ribonuclease mapping data support the form 1 and form 2 secondary structures suggested by the modification interference data. V1 cleavages occur primarily in helical regions while T1 and P1 cleavages occur in single-stranded regions. V1 nuclease cleavages seen at the 5′ end of the RNAs may result from overdigestion and secondary cleavages. (The cleavages highlighted are the result of repeated experiments with several form 1 and form 2 variants.)

shown). This is the expected result for stabilization of the splice site helix and absence of the tertiary structure.

Examination of melting curves for additional mutants in this region (Figure 8B) persuaded us, however, that the base pairing in and around the putative splice site helix has noncanonical features. For example, M8 and M10 contain C-C and U-C mismatches, respectively, in the splice site helix, yet the low-temperature melting transition is only slightly destabilized. On the other hand, the double mutant M9, in which the C-C and C-U mismatches are combined, has substantially altered properties. In an additional mutant, M4, we tried to incorporate a G-G mismatch in the splice site helix, with the result that the low-temperature transition was stabilized (data not shown). However, the Fold program in this case revealed an alternate pairing more stable than the splice site helix. The most likely general interpretation of these results is that the low-temperature signal of the WT RNA arises from cooperative melting of a structure that involves tertiary pairing of the 3′ end of form 1 RNA with a helix that has some but not all of the properties expected from the splice site helix. The single relaxation time, of rate slower than expected for melting helices joined by small loops, would thus be due to cooperative melting of multiple structural elements. Other methods, such as NMR spectroscopy, will be required to clarify the nature of the underlying structure.

Probing the Form 1 and Form 2 Structures with DNA Oligonucleotides. This set of experiments is similar to the oligonucleotide probing experiments described earlier. The oligonucleotide FORM1SS was designed to bind to the single-stranded region of form 1 while 5TAILD was designed to bind to the single-stranded region of form 2 (Figure 9). Melting curves were determined with the T-jump method because the DNA–RNA hybrids melt at a temperature which overlaps with the RNA tertiary structure melting signal. In an equilibrium melting experiment it is impossible to resolve these two signals, while in a T-jump experiment such resolution is feasible because the two types of melting occur on very different time scales: the RNA tertiary structure melts in about 100 μs, while the DNA–RNA hybrid melts on a 10–100-ms time scale. T-jump oligomer melting profiles were measured for both WT and M3 RNAs (form 1 and form 2, respectively).

The interaction of WT RNA with FORM1SS gives a large amplitude T-jump signal with a T_m of 45 °C, indicative of a

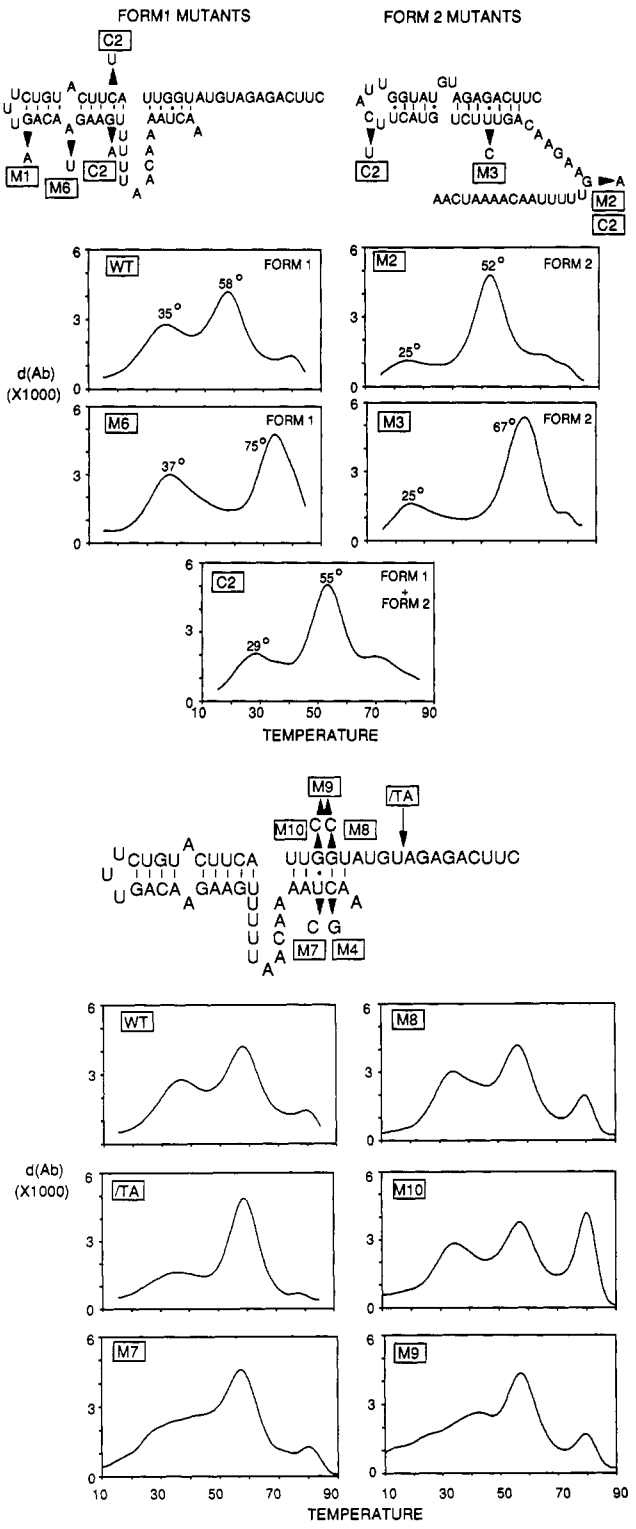

FIGURE 8: Differentiated thermal melting curves for SL 5′ half-mutants. (A, top) RNA mutations made in the core form 1 and form 2 helices. M2 takes on the form 2 structure by default because the form 1 structure is destabilized by an A-C mismatch. M3 takes on the form 2 structure because conversion of a G·U pair to G·C provides additional stability. C2 is a mixture of the two forms because form 2 is made less stable by conversion of a G·C pair to A·U. M6 has a greatly stabilized core helix because of repair of the A-A mismatch to an A·U base pair. (B, bottom) RNA mutations made in the putative splice site helix. The spectra shown are the first derivatives of the thermal melting profiles. All T_m's are taken as the maximum of the peaks in the differentiated curve. The melting temperatures below 70 °C show no dependence on concentration; the small peaks seen above 70 °C in some spectra are a result of aggregate formation of unknown origin.

strong interaction with a single-stranded region. The WT RNA was also probed with the form 2 specific oligonucleotide

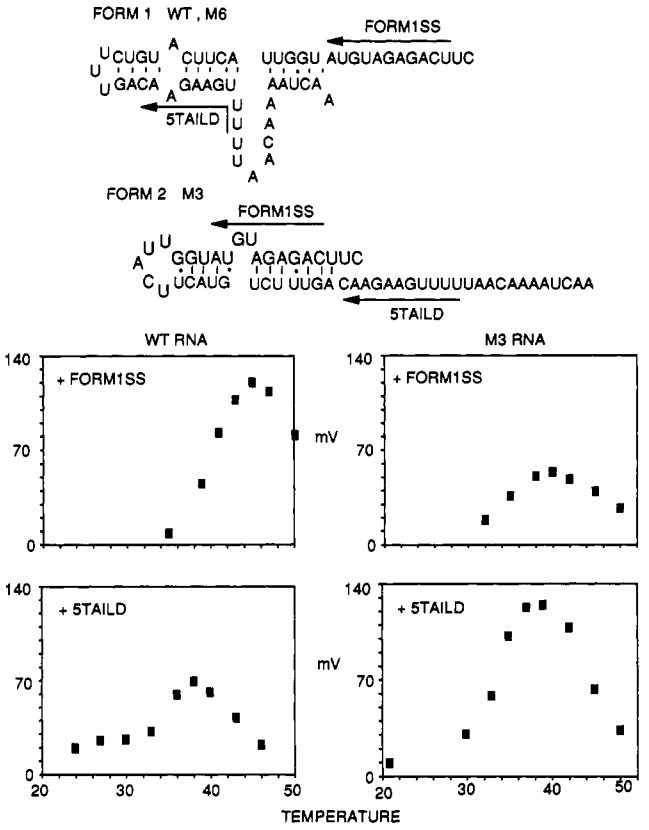

FIGURE 9: T-jump melting curves for the two forms of the SL RNA 5′ half interacting with form 1 and form 2 specific DNA oligonucleotides. FORM1SS is a 10-mer DNA oligonucleotide complementary to the single-stranded region of form 1 RNAs. 5TAILD is a 10-mer oligonucleotide complementary to the single-stranded region of form 2 RNAs. T-jump melting curves are shown for WT and M3 RNAs (form 1 and form 2) interacting with FORM1SS and 5TAILD oligonucleotides. Note the larger amplitude melting curves which correspond to the FORM1SS + WT and 5TAILD + M3 interactions, both cases in which the RNA should bind the oligonucleotide with no requirement for a conformational switch. Note that the apparent T_m values in the other two cases are perturbed by coupling to optical changes which accompany the switch between structural forms 1 and 2 and do not therefore provide a reliable guide to the stability of binding.

5TAILD. This oligonucleotide gives a medium amplitude signal with a T_m of 38 °C. Note that the form 2 binding oligonucleotide must perturb the form 1 RNA structure in order to bind, which it can do by one of two mechanisms: either by invading the structure or by switching the RNA conformation to form 2.

To distinguish these two possibilities, we used the truncated RNA /TA which is locked into the form 1 helix because it is missing bases essential for the form 2 helix. When 5TAILD is mixed with /TA RNA, no appreciable signal is measured, indicating that because this RNA cannot switch to the form 2 structure, the 5TAILD oligonucleotide is prevented from binding. We conclude that oligonucleotides bind the "wrong" form of the RNA by switching its conformation to that which is favorable for binding. Coupling of the conformational switch with oligonucleotide binding results in a reduced T-jump signal amplitude due to reduction of $\Delta H°$, the enthalpy change, and a decrease in $\Delta\epsilon$, the change in molar absorptivity. This experiment confirms that the structure of the 5′ half of the SL RNA is flexible and not rigidly locked into a single conformation.

Mutant M3 RNA, a form 2 RNA, was probed with the form 2 binding oligonucleotide 5TAILD. This oligonucleotide gives a large amplitude signal with a T_m of 40 °C. (Note that T_m values increase in proportion to the number of G·C pairs

in the hybrid helix.) The large signal amplitude is consistent with the oligonucleotide binding to an accessible region without requiring a conformational switch. Probing this form 2 RNA with the form 1 binding oligonucleotides FORM1SS gives a medium intensity signal with a T_m of 38 °C. Thus, the form 2 RNA M3 can bind to the form 1 specific oligonucleotides. Both T-jump and stopped-flow kinetic experiments (K. A. LeCuyer and D. M. Crothers, unpublished results) demonstrate that this binding event occurs by switching the RNA to a different (form 1) conformation. Again, the equilibrium for oligonucleotide binding is complicated by the competing equilibrium of the RNA conformational switch.

In the last set of experiments, the RNA mutant M6 was probed with both the form 1 and form 2 specific oligonucleotides (data not shown). M6 is a form 1 RNA with a very stable hairpin helix due to the repair of the A-A mismatch to an A·U base pair. The data for the form 1 binding oligonucleotide FORM1SS are comparable to that for WT. The 5TAILD oligonucleotide was modified to compensate for the M6 base change and then mixed with M6 RNA. The altered 5TAILD oligonucleotide gives no signal with the M6 RNA. The increased stability of the M6 helix must effectively lock the RNA into the form 1 structure and thus prevent form 2 specific oligonucleotides from binding, providing further confirmation of the conformational switch mechanism of oligonucleotide binding.

DISCUSSION

General Features of the Structure. T-jump melting experiments in which complementary DNA oligonucleotides were used to probe the full-length SL RNA indicate that the energy minimization results, as summarized in the model of Bruzik et al. (1988), give essentially the correct structure for the 3′ half but not for the 5′ half of the SL RNA. These experiments confirmed a consensus single-stranded Sm protein binding site flanked by two stem loops for the SL 3′ half. Probing the 5′ half of the SL RNA with oligonucleotides demonstrated that the structure in this part of the RNA is more complicated than that given by the Fold program but initially gave no interpretable evidence for what structures might be present.

Localization of the source of the low-temperature transition observed in the thermal unfolding curve for the full-length SL RNA was possible using long, complementary DNA oligonucleotides as blocking probes to hybridize to regions of the RNA structure. The results of this series of experiments allowed the assignment of the 33 °C signal to the 5′ half of the RNA, up to the 5′ end of helix 2, independent of the presence of the rest of the RNA. The higher temperature kinetically resolved signal was assigned as a composite of two helical stems, one in the 5′ half and one in the 3′ half. At this point we decided to focus our study on the 5′ half of the RNA because it contains the unexplained low-temperature melting signal as well as the splice site for the trans splicing reaction. A T-jump profile of the RNA 5′ half exhibits the 35 °C tertiary structure melting signal as well as the 58 °C helical stem melting signal.

Two Competing Secondary Structures. To examine the structure of the SL 5′ half, we designed point mutations with the objective of determining their effect on the melting behavior. In the first series of SL RNA variants, we noticed that some of the mutant RNAs have a very different electrophoretic mobility than the wild-type RNA on nondenaturing gels. We exploited this fortuitous result, using the difference in electrophoretic mobility of the two RNA forms to apply the modification/interference technique of structure probing. The results led to the proposal that there are two secondary structural forms of the SL RNA. The most stable form of the SL RNA, which we call form 1, incorporates a base-pairing scheme alternate to that given in the Bruzik et al. (1988) model. Form 2, the previously proposed structure, is a less stable structure seen in mutant RNAs as a result of either destabilizing the form 1 pairing or stabilizing base pairs in form 2. Ribonuclease mapping of the wild-type 5′ half and several structural mutants supports the proposed secondary structures for the two SL RNA forms.

An interesting feature of the proposed form 1 structure is the putative helix formed between a UUGGU across the splice site and an ACUAA at the 5′ end. These sequences and thus the potential base pairing are conserved for all of the trypanosome SL RNA sequences. Neither the nematode, trematode, nor *Euglena* SL RNA sequences can be folded into the form 1 structure, yet all of them retain the potential for base pairing between the splice site and the 5′ end. This observation coupled with the folding of all of the trypanosome SL RNAs into reasonable form 1 structures provides support for the form 1 structure and its splice site–5′ end helix.

Equilibrium melting experiments demonstrate why form 1 is the dominant structure. The wild-type form 1 helix has a T_m of 58 °C, while the wild-type form 2 helix has a T_m of 53 °C. The greater stability of the form 1 helical region, coupled with the presence of the tertiary structure, makes it the preferred form of the RNA. These experiments show that form 1 has a characteristic tertiary structure signal of unknown origin. Form 2 has only a small low-temperature melting signal of reduced T_m. The pseudoknot interaction probed with mutants M2 and C2 (Figure 4) may contribute to this signal.

To further verify the form 1 and form 2 secondary structures, we constructed short, complementary DNA oligonucleotides specific for the single-stranded regions of form 1 or form 2. The oligonucleotides specific for form 1 gave large differential absorbance melting signals with form 1 RNAs, and the oligonucleotides specific for form 2 gave correspondingly large differential profiles with form 2 RNAs. Surprisingly, mixing oligonucleotides with the "wrong" form of RNA, as in a form 2 binding oligonucleotide with a form 1 RNA, gave a melting signal indicative of binding but of medium intensity and with T_m values somewhat reduced. Further experiments demonstrated that this binding to the wrong form of the RNA is a result of an oligonucleotide-induced switch of the RNA conformation to a form which favors binding. Rather than being locked into a rigid conformation, the structure of the SL RNA is flexible and subject to perturbation from external factors. Mutations can fix the RNA in one form or the other and should thus allow further investigation into the structures of the two forms.

Tertiary Structure. The melting profile of the SL RNA 5′ half contains two melting signals, a low-temperature signal tentatively assigned to melting of tertiary structure and the putative splice site helix, and a higher temperature signal corresponding to the stable form 1 hairpin helix. The nature of the tertiary structure is not yet understood. The reduced amplitude of the low-temperature melting signal in the truncation mutant indicates that the 3′ single-stranded region of the form 1 structure is involved in tertiary interactions. This conclusion is supported by stopped-flow kinetic studies of binding oligonucleotides to the 3′ single-stranded region (K. A. LeCuyer and D. M. Crothers, unpublished results). Further mutagenesis will be necessary to determine which bases are critical for tertiary structure formation, and NMR studies of the structure are underway (K. Harris, J. Lapham,

and D. M. Crothers, unpublished results).

Dynamics of the Structural Switch. The T-jump technique was applied to address the time scale of the conformational switch. T-jump studies of the kinetics of oligonucleotide binding suggest that the oligonucleotide binding equilibrium is affected by the competing equilibrium for the RNA conformational switch when the switch is necessary for oligonucleotide binding (K. A. LeCuyer and D. M. Crothers, unpublished results). The time scale of the RNA conformational switch cannot be substantially slower than the time required for oligonucleotide binding, which we know occurs in a few hundred milliseconds. Stopped-flow experiments have also been used to confirm the time scale for the conformational switch (unpublished results). The rapid time scale of the interconversion suggests that it may occur by a branch migration pathway. For example, the potential pseudoknot interaction which links UGA in the 5′ tail to UCA in the form 2 loop (see Figure 4) provides a nucleus for the form 1 helix, which can then grow at the expense of the form 2 helix. Our detailed kinetic analysis (K. A. LeCuyer and D. M. Crothers, unpublished results) supports the existence of such intermediates.

A Possible Functional Role of the Structural Switch. A variety of techniques have been used to refine the structure of the *L. collosoma* SL RNA. The role of both the tertiary structure and the two conformations of the RNA in the mechanism of trans splicing has yet to be identified. It should be stressed that the nearly equal stabilities of SL RNA forms 1 and 2 mean that either could be the thermodynamically favored form in the particle. In this connection we note that the putative splice site helix is in the region of the RNA which undergoes the switch, and Steitz (1992) has proposed a model that has pairing at the splice site which incorporates features of both models. It is also worth noting that in the previously proposed structure, which we call form 2, the intron is extensively paired with the sequences from which it must subsequently be removed. The form 1 structure, however, has virtually no base pairing between the 5′ spliced leader and the intron which is removed from the SL RNA. Thus one possible role for the conformational switch may be to provide a mechanism to disrupt base pairing between the mRNA and the SL RNA intron, acting effectively as a helicase.

Analogies to RNA–RNA Interactions in Mammalian Splicing Systems. Trans splicing in trypanosomes is clearly evolutionarily related to mRNA splicing, although there are some evident differences. For example, U1 RNA, whose 5′ end pairs with the 5′ splice site in mammals (Zhuang & Wiener, 1986), is missing in trypanosomes (Mottram et al., 1989). Furthermore, SL RNA sequences can substitute for the essential U1 function in mammalian splicing (Bruzik & Steitz, 1990). In addition, the modifications to bases at the 5′ end of SL RNA are analogous to those at the 5′ end of U1 RNA (Ullu & Tschudi, 1991). Our observation that the 5′ end of SL RNA appears to pair with the SL splice site, albeit with nonstandard features, suggests that this is how the U1 function is provided, thus enabling a single RNA to combine multiple functions of the mammalian splicing machinery. A further possible analogy is based on the apparent interaction of yeast U5 RNA with the 5′ splice site (Newman & Norman, 1991); U5 appears also to be missing in trypanosomes (Mottram et al., 1989). In the model proposed by Steitz (1992), the U5 function results from combining the form 1 and form 2 pairings at the splice site. It is also possible that the tertiary interactions which we observe are somehow related to the U5 or another splicing interaction. Thus the SL RNAs incorporate important models for critical RNA–RNA interactions at the splice site.

REFERENCES

Blumenthal, T., & Thomas, J. (1988) *Trends Genet. 4*, 305–308.
Bruzik, J. P., & Steitz, J. A. (1990) *Cell 62*, 889–899.
Bruzik, J. P., Van Doren, K., Hirsh, D., & Steitz, J. A. (1988) *Nature 335*, 559–562.
Celander, D. W., & Cech, T. R. (1990) *Biochemistry 29*, 1355–1361.
Cole, P. E., & Crothers, D. M. (1972) *Biochemistry 11*, 4368–4374.
Conway, L., & Wickens, M. (1989) *Methods Enzymol. 180*, 369–379.
Crothers, D. M., Cole, P. E., Hilbers, C. W., & Shulman, R. G. (1974) *J. Mol. Biol. 87*, 63–88.
Douthwaite, S., & Garrett, R. A. (1981) *Biochemistry 20*, 7301–7307.
Gralla, J., Steitz, J. A., & Crothers, D. M. (1974) *Nature 248*, 204–208.
Konarska, M. M., Padgett, P. A., & Sharp, P. A. (1985) *Cell 42*, 165–171.
Kraus, M., & Hirsh, D. (1987) *Cell 49*, 753–761.
Lerner, M. R., & Steitz, J. A. (1979) *Proc. Natl. Acad. Sci. U.S.A. 76*, 5495–5499.
Maniatis, T. M., & Reed, R. (1987) *Nature 325*, 673–678.
Mattaj, I. W. (1988) U snRNP assembly and transport, in *Structure and Functions of Major and Minor Small Nuclear Ribonucleoprotein Particles* (Birnstiel, N. L., Ed.) pp 100–114, Springer-Verlag, Berlin.
Milligan, J., Groebe, D. R., Witherall, G. W., & Uhlenbeck, O. C. (1987) *Nucleic Acids Res. 15*, 8783–8798.
Mottram, J., Perry, K. L., Lizardi, P. M., Lührman, R., Agabian, N., & Nelson, R. G. (1989) *Mol. Cell. Biol. 9*, 1212–1223.
Murphy, W. J., Watkins, K. P., & Agabian, N. (1986) *Cell 47*, 517–525.
Newman, A., & Norman, C. (1991) *Cell 65*, 115–123.
Padgett, P. A., Konarska, M. M., Grabowski, P. J., Hardy, S. F., & Sharp, P. A. (1986) *Annu. Rev. Biochem. 55*, 1119–1150.
Peattie, D. (1979) *Proc. Natl. Acad. Sci. U.S.A. 76*, 1760–1764.
Rajkovic, A., Davis, R. E., Simonsen, J. N., & Rottman, F. M. (1990) *Proc. Natl. Acad. Sci. U.S.A. 87*, 8879–8883.
Steitz, J. A. (1992) *Science 257*, 888–889.
Sutton, P. E., & Boothroyd, J. C. (1986) *Cell 47*, 527–535.
Takacs, A. M., Denker, J. A., Perrine, K. G., Maroney, P. A., & Nilsen, T. W. (1988) *Proc. Natl. Acad. Sci. U.S.A. 85*, 7932–7936.
Tessier, L.-H., Keller, M., Chan, R. L., Fournier, R., Weil, J.-H., & Imbault, P. (1991) *EMBO J. 10*, 2621–2625.
Turner, D. H. (1986) Temperature-jump methods, in *Investigation of Rates and Mechanisms of Reactions* (Bernasconi, C. F., Ed.) pp 141–189, Wiley, New York.
Ullu, E., & Tschudi, C. (1991) *Proc. Natl. Acad. Sci. U.S.A. 88*, 10074–10078.
Weeks, K. M., Ampe, C., Schultz, S. C., Steitz, T. A., & Crothers, D. M. (1990) *Science 249*, 1281–1285.
Zhuang, Y., & Weiner, A. M. (1986) *Cell 46*, 827–835.
Zuker, M. (1989) *Science 244*, 48–52.